PHYSICAL REVIEW B **67**, 201402(R) (2003)

Single-atom manipulation mechanisms during a quantum corral construction

Saw-Wai Hla*
Nanoscale & Quantum Phenomena Institute, Physics & Astronomy Department, Ohio University, Athens, Ohio 45701

Kai-Felix Braun and Karl-Heinz Rieder
Institut für Experimentalphysik, Freie Universität Berlin, D-14195 Berlin, Germany
(Received 21 January 2003; published 27 May 2003)

We describe a complete picture of how single Ag atoms move on the various potential energy landscapes of an Ag(111) surface during a quantum corral construction by using a scanning tunneling microscope (STM) tip at 6 K. The threshold tunneling resistance and tip-height to move the Ag atom across the surface are experimentally measured as 210 ± 19 kΩ and 1.3 ± 0.2 Å. The experimental atom manipulation signals reveal remarkably detailed atom movement behaviors dependent on the surface crystallographic orientation and offer atomic-level tribology information.

DOI: 10.1103/PhysRevB.67.201402 PACS number(s): 81.16.Ta, 46.55.+d, 68.37.Ef, 85.35.−p

Bottom-up approach is one of the main focus research areas of nanoscience[1,2] where various atomic structures will be constructed on an atom-by-atom basis. Manipulation with a scanning tunneling microscope (STM) tip allows engineering of man-designed structures using single atoms/molecules or investigating the physical/chemical properties of materials at an atomic level.[1–11] Positioning of single atoms with sub-atomic level precision on a surface requires an extremely fine control over the tip-atom-surface junction. The detailed knowledge of how an atom moves across a surface is valuable for both fundamental understanding and further progress of nanoscience.

The experiments were conducted by using a low temperature UHV-STM operated at ~6 K. The Ag(111) surface was cleaned by repeated sputter-anneal cycles.[7] An etched W wire was used as the STM tip. Single Ag atoms for the experiment are produced in situ by manipulating the native substrate with the tip. The detailed tip preparation and in situ single atom production procedures will be published elsewhere. To construct the quantum corral, Ag atoms are relocated on the surface using the lateral manipulation procedure.[2,12–15] It involves approaching the tip toward the atom and then moving the tip along a chosen path in a constant current mode. At the final destination, the tip is retracted back to the initial imaging height leaving the atom at the desired location on the surface.

To investigate the tip-atom interaction responsible for the manipulation process, the tunneling resistance necessary to move the atom was first determined. We have developed a computer controlled automated-manipulation scheme for this purpose. Initially, the computer automatically located the position of a single atom, and then the atom was moved across the surface to a random final location selected by the computer. For each bias, the atom was manipulated by using different current values (from 8 to 950 nA). For each set of current and bias, 24 or more manipulations were done. Figure 1(a) shows the manipulation probability vs tunneling current plot at −45 mV. In this bias, the probability changes from 0 (below 147 nA) to 1 (above 250 nA). The average threshold current is determined to be 200 nA.

By changing the bias, the entire procedure is repeated. An extensive set of 3857 computer-automated measurements has been taken for the bias range from ±10 to ±55 mV. Evaluation of these data yields the minimum current necessary to move the atom as a function of the bias averaged over all surface directions. Figure 1(b) depicts the results, which clearly display a linear dependence between the tunneling voltage and the threshold current, independent of the bias polarity. Each data point here is determined by plotting a curve as in Fig. 1(a). From the slope of the curve, a tunneling resistance (R_t) of 210 ± 19 kΩ has been measured [Fig. 1(b)]. This linear relationship indicates that the R_t is the ultimate matter to move an atom within the bias range used. The tip-surface distance is calibrated by measuring R_t as a function of tip-height [Fig. 1(c)]. This is accomplished by acquiring the IZ spectroscopy. The calibration reveals that the R_t of 210 kΩ corresponds to a distance of 1.3 ± 0.2 Å [Fig. 1(c)]. Due to this close distance, we estimate that chemical nature of tip-atom interaction is the main driving force in our manipulation process.

During the circular quantum corral (Fig. 2) construction, the tip speed is fixed at 10 Å/s. We use $R_t = 15$ kΩ, which is well below the measured threshold value. At this distance, the tip is in almost mechanical contact with the atom. The manipulation paths are precisely determined on the basis of atomic resolution STM images of the surface. Because the thermal drift of our STM is less than 1 Å/hr at 6 K, we are able to manipulate atoms back and forth on the same manipulation path for many times. To ensure reproducibility we repeat the manipulation at least ten times for each path, totaling over 360 manipulations for the corral construction alone. In addition, atom manipulations are also performed at separate locations to verify the specific features observed in the manipulation signals.

Initially each atom was positioned at the center of the corral [Figs. 2(a) and 2(c)] and then relocated to a final position. The manipulation path of the first atom was chosen along a surface atomic close-packed (CP) row [Fig. 2(c)], i.e., along [110]. Then the next atoms were moved along a direction 10° rotated from the previous paths [Figs. 2(c) and 2(d)]. Thus a total of 36 atoms are required for 360° to com-

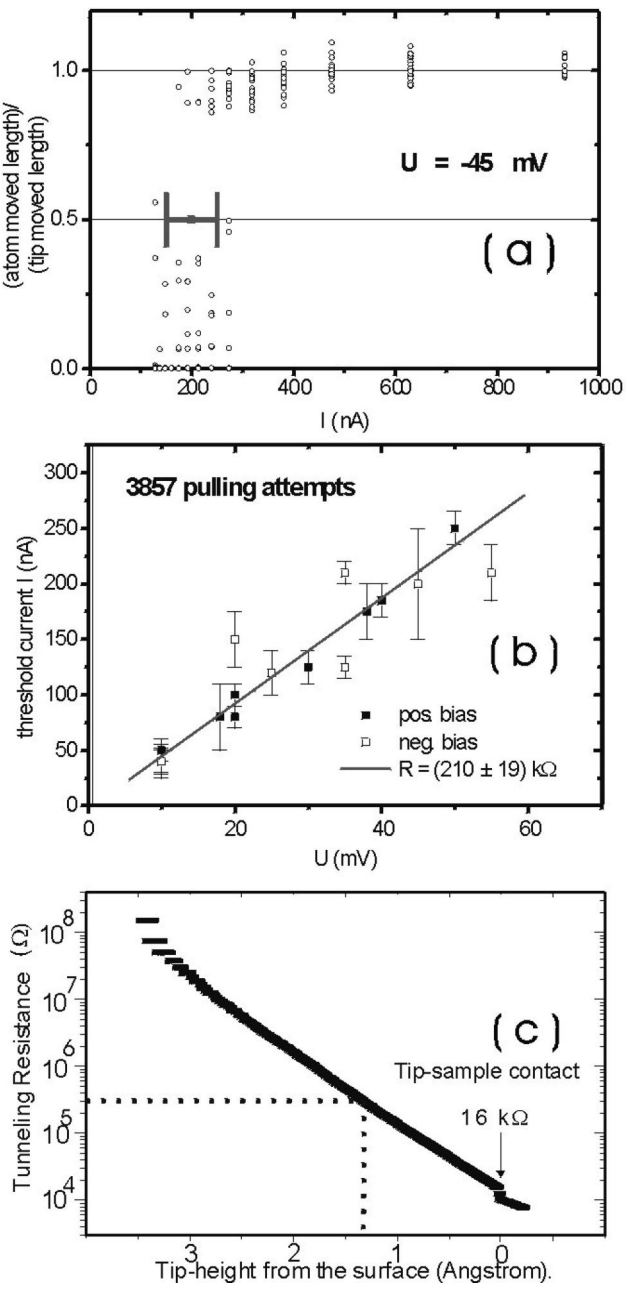

FIG. 1. Tunneling resistance (R_t) for a successful atom manipulation. (a) The probability of moving an Ag atom vs tunneling current at −45 mV. (b) The measured threshold current, accumulated from 3857 automated atom-manipulations, reveals its linear dependence on the tunneling voltage. (c) The R_t vs tip-height on an Ag(111) surface at 46 mV bias. The ohmic-contact (tip-surface contact) point is indicated with an arrow. Dashed lines are drawn to guide the threshold R_t to move an atom and the corresponding tip-height.

plete a circle. For simplicity, we will discuss the various tip-paths as a function of deviation angle θ from the CP rows [Fig. 2(d)]. On an fcc(111) surface, CP rows are located at every 60° [Fig. 2(d)]. In addition, because of the surface mirror symmetry, the tip-paths for θ=10° and 50° and for θ=20° and 40° encounter the same surface geometry [Fig. 2(d)]. Thus analyses on the atom movements between θ=0° and 30° tip-paths are sufficient to cover all surface directions.

The atom moves in the pulling mode[13,14] along the CP rows (θ=0°) indicating the attractive tip-atom interaction.[12] The 2.89 Å hop length (Fig. 3) shows that it visits only one kind of site, either hcp or fcc, upon following the tip. Due to a lower diffusion barrier, the CP rows are the most favored atom-traveling paths.[12,16] Complex manipulation signals are observed when the paths deviate from the CP rows. Fig. 3 collects experimental atom manipulation signals along various tip-paths.

In the 10° tip-path, the manipulation signals include smaller steps (Fig. 3) caused by the atom visiting both fcc and hcp sites (Fig. 4). This is induced due to a slight lateral displacement of the tip-apex to the left or right side of the CP row where the atom is traveling (Fig. 4), but the tip is still in close proximity to the atom.[12] As the tip continues to move along its 10° path, the atom follows the tip by traveling along the CP row (Fig. 4). Due to different directions, the tip-atom distance increases and the tip-atom interaction reduces. Finally, the atom is traveling by visiting only single sites, either fcc or hcp again (larger steps). Continuation of the tip movement along the 10° path leads to a further increase in the tip-atom distance. Since now the atom is no longer directly located under the tip-apex, the tip moves closer to the surface. This increases the lateral force component, F_x (Fig. 4). When F_x is large enough to overcome the surface potential barrier, the atom hops to the next CP row to follow the tip. Now it is in close proximity to the tip-apex again. From that point another series of single and hcp-fcc sites traveling sequences is repeated.

A different kind of manipulation signal is observed when manipulated along the θ=20° tip-path (Fig. 3). The distinctive features in this signal are the periodic deep slopes. The specific atom movement can be perceived as follows: When θ becomes larger, the intersection time between the tip-path and the adjacent surface CP rows becomes shorter. Yet the atom still prefers to travel along the CP row and in doing so it moves away from the tip shortly after such an intersection (Fig. 4). At one point it can no longer continue to move along the CP row because of the large tip-atom distance. Then the atom stops traveling and rests for some time, as if it is unsure what to do next (Fig. 4). This behavior can be regarded as a competition between the atom's preference to travel along the CP row and its duty to follow the tip. The tip continues its scan by following the downslope of the now resting atom's edge that results in the falling of the tip-height to a lower value (Fig. 3) and thereby increases the lateral force, F_x. When F_x overcomes the hopping barrier, the atom jumps back under the tip which is now already above the next CP row. This hopping alerts the STM feedback system to retract the tip resulting in a rapid increase of the tip-height signal (Figs. 3 and 4). The atom travels by repeating this ''move-rest-jump'' cycle.[17]

When θ=30°, the tip-path no longer intersects with the CP rows [Fig. 2(b)]. Thus the atom cannot follow the tip by traveling along a CP row. The surface geometry along this path includes repeating units of three hollow sites. The first

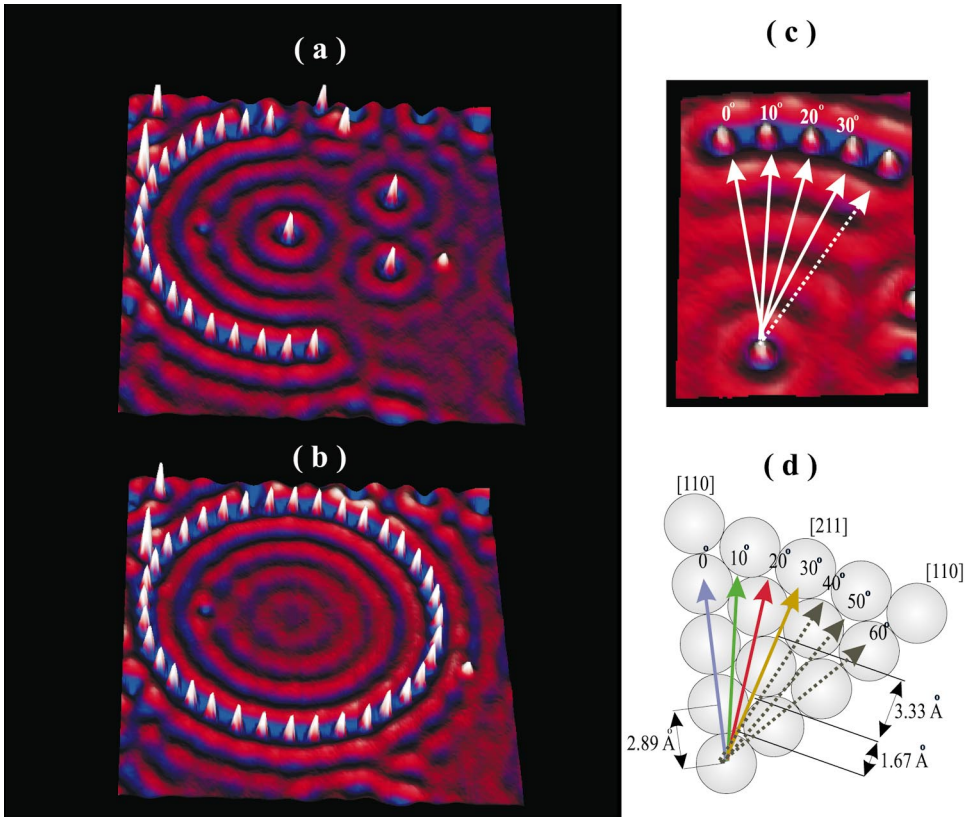

FIG. 2. (Color) Quantum corral construction. 3D STM images show (a) during construction and (b) after completion of the corral. 36 Ag atoms (white protrusions) are used (diameter=31.2 nm). A STM image (c) and a sphere model (d) demonstrate the tip-paths and the surface geometry encountered during manipulations.

two sites, *a* and *b*, are 1.67 Å apart, and the third site *c* is 3.33 Å from *b* [Figs. 4 and 2(b)]. The atom moves in a sliding mode[13,14] between *a* and *b* producing two smooth bumps 1.7 Å apart in the signal (Figs. 3 and 4). It does not travel directly from *b* to *c* due to a higher hopping barrier caused by a relatively far distance between these two sites. The theory predicts the nearest and the next nearest local minimum energy locations for the atom as the two adjacent hollow sites, *d* and *e* (Fig. 4).[12] The manipulation signal shows that after moving the downslope of the atom contour at site *b*, the tip starts to climb up the new atom contour which belongs to the site *c* (Figs. 3 and 4). This indicates that the atom has already moved in front of the tip. Instead of moving straightforwardly along the tip-path, the atom finds its way to the site *c* by smoothly sliding through the two nearby sites *d* and *e* resulting in an approximate semicircle traveling path (Fig. 4).[17] In this way it avoids entering under the tip-apex and thus, no apparent signature can be observed in the manipulation signal. To further support these atom movement behaviors, we have manipulated Ag atoms along $\theta=5°$, 15°, and 25° tip-paths, halfway between the angles we discuss above. At $\theta=5°$, the tip remains in a close proximity to the CP row for a longer time than at $\theta=10°$. As a result, the number of smaller steps (hcp-fcc hopping) is increased in this path. The manipulation signal for $\theta=15°$ (Ref. 17) shows similar structure as for $\theta=20°$ with a reduced frequency of deeper slopes. At $\theta=25°$, the manipulation signals consist of mixed features from the 20° and 30° paths. Even though we used a fixed tip-sample distance and the same tip speed for all the atom manipulations described above, the atom movement styles are completely different and dependent on the surface potential-energy landscapes. A sudden transition from a pronounced discontinuous movement at $\theta=20°$ path to a smooth sliding movement at $\theta=30°$ path occurs.[17] This shows that at the atomic scale the surface

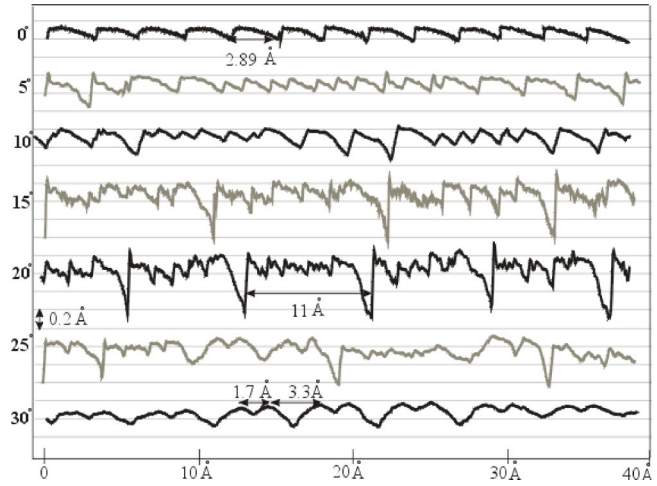

FIG. 3. Single-atom manipulation signals. $\theta=0°$ signal shows pulling mode with the single-site atom hops (2.89 Å). At $\theta=5°$, small steps at the middle part is due to fcc-hcp site-visiting of the atom. In $\theta=10°$ signal, two series of small steps are separated by large steps in between. At $\theta=15°$, the periodic appearance of the deep downslopes followed by a rapid tip-height increase is due to the resting and then jumping of the atom to the next CP row. The ''rest-jump'' circle frequency increases at $\theta=20°$. The $\theta=30°$ signal includes two consecutive bumps (1.7 Å apart) followed by the next pair with 3.3 Å. At $\theta=25°$, the manipulation signal reveals both structures of $\theta=20°$ and 30°.

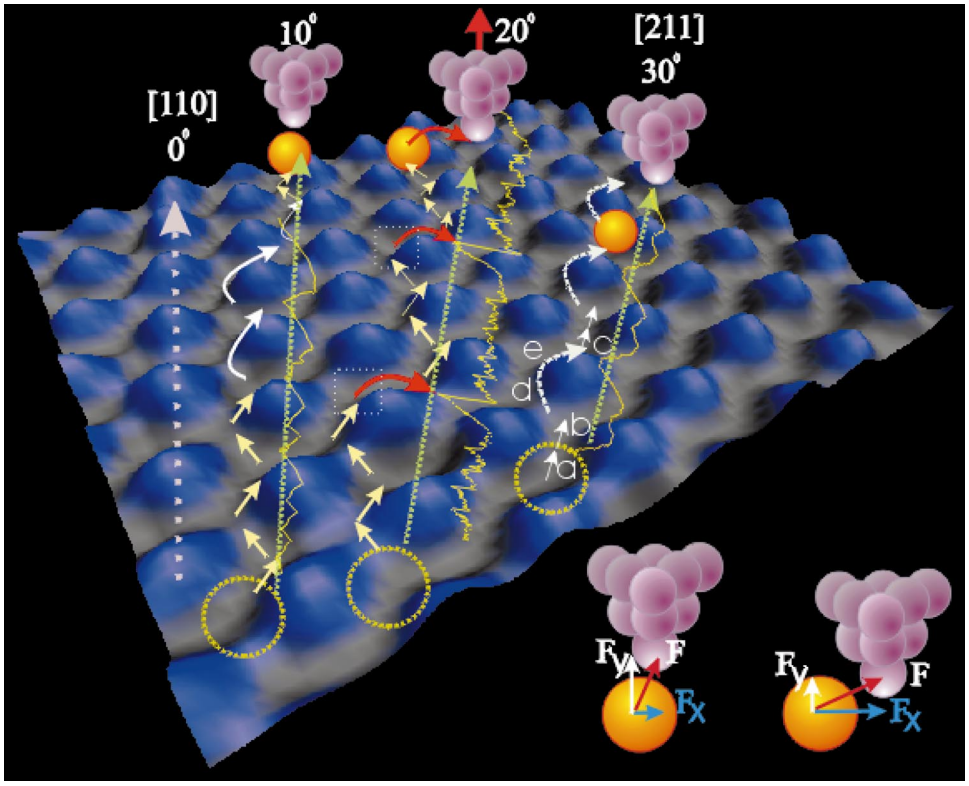

FIG. 4. (Color) Detailed atom movement mechanisms. The atom movements along various tip-paths are demonstrated by super exposing an actual 3D STM image of the Ag(111) with the manipulation signals. The atom briefly rests at the square locations in the 20° path. When lateral force component F_x (lower right drawings) exceeds the hopping barrier, the atom jumps to the adjacent CP row (shown by red arrows) to follow the tip. At the 30° path, the atom sides to the first two sites *a* and *b* producing two consecutive bumps in manipulation signals (Fig. 3). It then travels through the sites *d* and *e* to reach the site *c*. The two drawings in the lower right corner demonstrate that the magnitude of F_x is dependent on the tip positions.

potential-energy configuration plays a key role in tribology aspects.

In summary, our experimental report yields intimate details of atom movement mechanisms as well as atomic level tip-atom interaction during STM manipulations and provides an important step forward for the progress of the bottom-up approach in nanoscience. This project was partly funded by DFG RI 472/3-2, SFB 290/TPA5 (KFB, KHR), and United States Department of Energy, BES, DE-FG02-02ER46012 (SWH) grants.

*Corresponding author. Email: hla@helios.phy.ohiou.edu, Web: www.phy.ohiou.edu/~hla

[1] C. Joachim, J. K. Gimzewski, and A. Aviram, Nature (London) **408**, 541 (2000).
[2] S. W. Hla and K.-H. Rieder, Superlattices Microstruct. **31**, 63 (2002).
[3] J. K. Gimzewski and C. Joachim, Science **283**, 1683 (1999).
[4] H. C. Manoharan, C. P. Lutz, and D. M. Eigler, Nature (London) **403**, 512 (2000).
[5] M. F. Crommie, C. P. Lutz, and D. M. Eigler, Science **262**, 218 (1993).
[6] S.-W. Hla *et al.*, Phys. Rev. Lett. **85**, 2777 (2000).
[7] K.-F. Braun and K.-H. Rieder, Phys. Rev. Lett. **88**, 096801 (2002).
[8] G. Dujardin *et al.*, Phys. Rev. Lett. **89**, 036802 (2002).
[9] S. Heinze *et al.*, Phys. Rev. Lett. **89**, 106801 (2002).
[10] T. W. Fishlock *et al.*, Nature (London) **404**, 743 (2000).
[11] M. R. Falvo *et al.*, Nature (London) **389**, 582 (1997).
[12] A. Kühnle *et al.*, Surf. Sci. **499**, 15 (2002).
[13] L. Bartels, G. Meyer, and K. H. Rieder, Phys. Rev. Lett. **79**, 697 (1997).
[14] X. Bouju, C. Joachim, and C. Girard, Phys. Rev. B **59**, R7845 (1999).
[15] U. Kurpick and T. S. Rahman, Phys. Rev. Lett. **83**, 2765 (1999).
[16] J. Li, R. Berndt, and W.-D. Schneider, Phys. Rev. Lett. **76**, 1888 (1996).
[17] See EPAPS Document No. E-PRBMDO-67-R18316 for animation movies of the atom movement mechanisms. A direct link to this document may be found in the online article's HTML reference section. The document may also be reached via the EPAPS homepage (http://www.aip.org/pubservs/epaps.html) or from ftp.aip.org in the directory /epaps/. See the EPAPS homepage for more information.